Journal of Molecular Liquids 360 (2022) 119440

Contents lists available at ScienceDirect

Journal of Molecular Liquids

journal homepage: www.elsevier.com/locate/molliq

Thermodynamic descriptors of sensible heat driven liquid-liquid phase separation

Sidharth Sanadhya [a], Zachary D. Tucker [b], Eva M. Gulotty [b], William Boggess [b], Brandon L. Ashfeld [b,*], Saeed Moghaddam [a,*]

[a] Department of Mechanical and Aerospace Engineering, University of Florida, Gainesville, FL 32608, USA
[b] Department of Chemistry and Biochemistry, University of Notre Dame, Notre Dame, IN 46556, USA

ARTICLE INFO

Article history:
Received 3 April 2022
Revised 17 May 2022
Accepted 20 May 2022
Available online 25 May 2022

Keywords:
Critical Temperature
Ionic Liquids
Thermodynamic Stability
Gibbs Energy
Activity Coefficient

ABSTRACT

Separation of a homogeneous solution into its constituent liquids through sensible heating obviates the need for vaporization/distillation and the associated latent heat of phase change. Therefore, it could enable alternative more energy efficient cycles in many applications that involve the separation of miscible liquids. This can be achieved by utilizing Lower and Upper Critical Solution Temperature (LCST/UCST) driven phase separation. This study identifies the thermodynamic descriptors for predicting LCST/UCST exhibiting ionic liquid (IL) - water/alcohol (solvent) solutions, and therefore provides a fundamental insight into the underlying energetics responsible for temperature and concentration dependent miscibility of multicomponent solutions. Excess Gibbs energy analysis of 50 solutions revealed that the solvent (water/alcohol) played a pivotal role in phase separation and exhibited contrasting excess Gibbs energy contributions in the LCST and UCST regimes. Furthermore, analysis of scaled Gibbs energy was carried out to elucidate the energetics of phase separation and differentiate between LCST and UCST thermodynamically. Consequently, we introduce the solvent Reduced Activity Coefficient (RAC) which was used to successfully predict the phase separation behavior without evaluating the Gibbs energy function, thus saving significant computation time.

1. Introduction

Thermally driven separation processes such as distillation, evaporation, and drying require significant latent and sensible heat inputs. Hence, these processes account for a substantial share of the total separation energy consumed in different industrial applications, of which, the primary component is that of the latent heat energy required for vaporization [1,2]. Other applications that consume significant latent heat include building dehumidification, absorption cooling, thermal desalination, etc. [3,4]. Therefore, development of alternative separation processes driven by sensible heat could result in significant energy savings [1] and production of food and materials with less pollution, waste, and adverse climate impact.

Phase separation through LCST/UCST is a known phenomenon that constitutes the basis of the principle described above. In the case of LCST, a homogenous liquid solution undergoes phase separation by increasing the solution temperature. For UCST, on the other hand, a decrease in solution temperature leads to phase separation. Notably, this type of phase separation results in immiscible liquid phases without vaporization or latent energy consumption. An example of such a thermoresponsive biphasic system (IL + water) is depicted in Fig. 1, in which phase separation is achieved without vaporizing the solvent (water). However, a fundamental prerequisite needs be fulfilled to implement and extend this phenomenon to applications of scientific and industrial significance. That being, the predictive estimation of phase separation behavior from solute-solvent molecule structures and an elucidation of the associated thermodynamics of the solution. Determining these factors would foster the molecular engineering of task specific solute–solvent pairs required for LCST/UCST driven separation processes.

Reports of LCST/UCST behavior in hydrocarbon mixtures date back to 1911, and subsequent studies have revealed similar phase separation behavior for alcohols, polymers, and ionic liquids [5–8]. Recent studies by Fukumoto and Ohno have shown that a select

* Corresponding authors.
E-mail addresses: bashfeld@nd.edu (B.L. Ashfeld), saeedmog@ufl.edu (S. Moghaddam).

https://doi.org/10.1016/j.molliq.2022.119440
0167-7322/

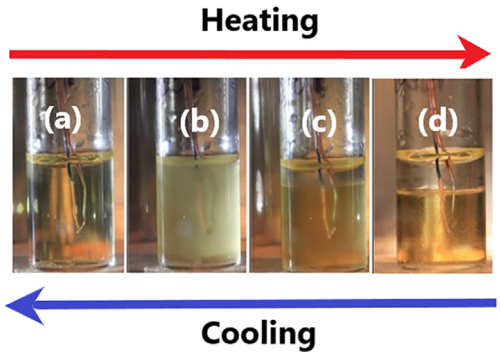

Fig. 1. LCST driven liquid–liquid phase separation exhibited by aqueous [P_{4444}][TOS] (Tetrabutylphosphonium p-Toluenesulphonate) solution (50% w/w).**(a)** homogenous solution at room temeprature **(b)** cloud phase **(c)** onset of separation **(d)** separation complete at 37 ^{0}C.

few ILs, exhibited LCST behavior with water [9–12]. Heuristics have been developed to rationalize LCST behavior in aqueous IL solutions based on an empirical "hydrophilicity index" (HI), which represents the number of water molecules per ion pair in the IL-rich phase upon phase separation [13]. With notable exceptions to this heuristic [14,15], a quantitative method of assessing HI *a priori* remains elusive, and the HI of a given IL-water pair is determined only after synthesis, formulation, and experimental testing. Ultimately, this approach limits the efficiency with which ILs are developed to meet the stringent performance attributes required to develop industrially useful liquid–liquid separation processes. Moreover, these heuristics are not applicable to UCST exhibiting solutions and to solvents other than water, such as alcohols. Similar studies also rule out the possibility of predicting LCST/UCST behavior, at large [16].

To address these challenges, three predictive metrics based on excess Gibbs energy, Gibbs stability criterion and solvent activity coefficient have been discussed which characterize solution concentration and temperature dependent miscibility. The thermodynamic stability criterion established by the J.Willard Gibbs in his seminal work has been modified to incorporate temperature dependence and analytically evaluated in LCST and UCST regimes [17]. Finally, we have described a simplified solution stability criterion that can predict LCST/UCST behavior based on a single solution parameter i.e. the reduced activity coefficient (RAC).

The default concentration unit used in this study is the water mole fraction (x_W). However, all the images/figures also have corresponding graphs with water mass fraction (m_W) as the concentration unit and error analysis in the Supplementary Information (Refer SI pp.10). For the tabulated list of 50 IL-water/alcohol pairs with their respective molecular structures please refer SI pp. 13–21. Thermodynamic analyses for these IL-water/alcohol pairs have also been provided in the SI (pp. 25 onwards). For detailed IL synthesis procedure and NMR characterization please refer SI (pp. 84 onwards).

2. Excess Gibbs energy analysis

The formulation of predictive metrics for phase separation/homogenization inevitably follows from the Gibbs energy function of a real solution:

$$G_{sol} = \sum_i x_i g_i + RT \sum_i x_i ln(x_i) + RT \sum_i x_i ln\,(Y_i) \quad \text{(i)}$$

where x_i is the mole fraction of the i^{th} component, g_i is the pure component Gibbs energy, Υ_i is the activity coefficient of the i^{th} component in the solution. Eq. (i) can be rewritten as Eq. (ii) to give the Gibbs energy of mixing of the solution:

$$G_{mix} = G_{sol} - \sum_i x_i g_i = RT \sum_i x_i ln(x_i) + RT \sum_i x_i ln\,(Y_i) \quad \text{(ii)}$$

Furthermore, (ii) can be rewritten in the non-dimensional form as [18]:

$$G_{mix}/RT = (G_{sol} - \sum_i x_i g_i)/RT = \sum_i x_i ln(x_i Y_i) \quad \text{(iii)}$$

For a homogeneous solution to become unstable, following condition must be satisfied [18]:

$$G_{mix}/RT > 0 \quad \text{(iv)}$$

Unmixing or phase separation will be spontaneous for Temperature – Composition (T-x) values which satisfy this condition. From Eq. (ii) and (iii), it can be noted that the non-dimensional mixing Gibbs energy function for a real solution is composed of two parts, the ideal mixing component ($\sum_i \boldsymbol{x_i ln(x_i)} = \boldsymbol{G^{id}_{mix}/RT}$) and the excess component ($\boldsymbol{\sum_i x_i ln(Y_i) = G_{ex}/RT}$). As mole fraction ($x_i$) is always less than unity, $\boldsymbol{G^{id}_{mix}/RT}$ is always negative. Thus, mixing is favored at all compositions and temperatures in an ideal solution. Consequently, the ideal component always contributes toward stabilizing the homogeneous phase in a real solution. For an ideal binary solution, *A-B* composed of pure components *A* and *B*, all three interactions *A-A, B-B,* and *A-B* are equally favored at all compositions [19].

The deviation from ideal solution behavior, is accounted for by the excess component and it is a function of the activity coefficients of the respective components in the solution. A positive deviation implies that the pure component interactions (*A-A* and *B-B*) are favored over the dissimilar component interaction (*A-B*). This results in destabilization of the homogeneous solution leading to phase separation [20]. With this understanding, we analyzed aqueous solution of the IL [N_{4444}][SCN] (Fig. 2), which exhibits both LCST and UCST behavior [8].

T-x regimes wherein the homogenous solution is unstable can be clearly observed in Fig. 3(a) and (b). This region represents a closed loop phase diagram, a typical characteristic of binary solutions exhibiting sequential LCST and UCST, as the solution temperature is increased. Furthermore, the simulation results depicted in Fig. 3(a) and (b) are in good agreement with the experimental results [8].

Given the fact that an ideal solution cannot exhibit phase separation (Refer SI pp. 2), the positive contribution to total solution Gibbs energy of mixing ($\boldsymbol{G_{mix}/RT}$) and hence the phase separation behavior emanates entirely from the excess component. Therefore, to delineate the respective contributions in destabilizing the homogeneous solution, excess Gibbs energy of water ($\boldsymbol{G_{ex}(w)/RT}$) and that of the IL ($\boldsymbol{G_{ex}(IL)/RT}$) have been plotted in Fig. 3(c) and (d).

Within the unstable region of the LCST regime, it can be noted that $\boldsymbol{G_{ex}(w)/RT}$ and $\boldsymbol{G_{ex}(IL)/RT}$, both increase with the increase in temperature. This entails *IL-IL* and *W-W* interactions are favored over *IL-W* interactions as the temperature is increased, consistent with LCST driven phase separation. $\boldsymbol{G_{ex}(w)/RT}$ and $\boldsymbol{G_{ex}(IL)/RT}$ attain their respective maxima approximately at the same temper-

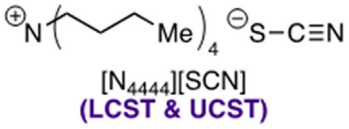

Fig. 2. Structure of the IL [N_{4444}][SCN] (Tetrabutylammonium Thiocyanate) used in this study.

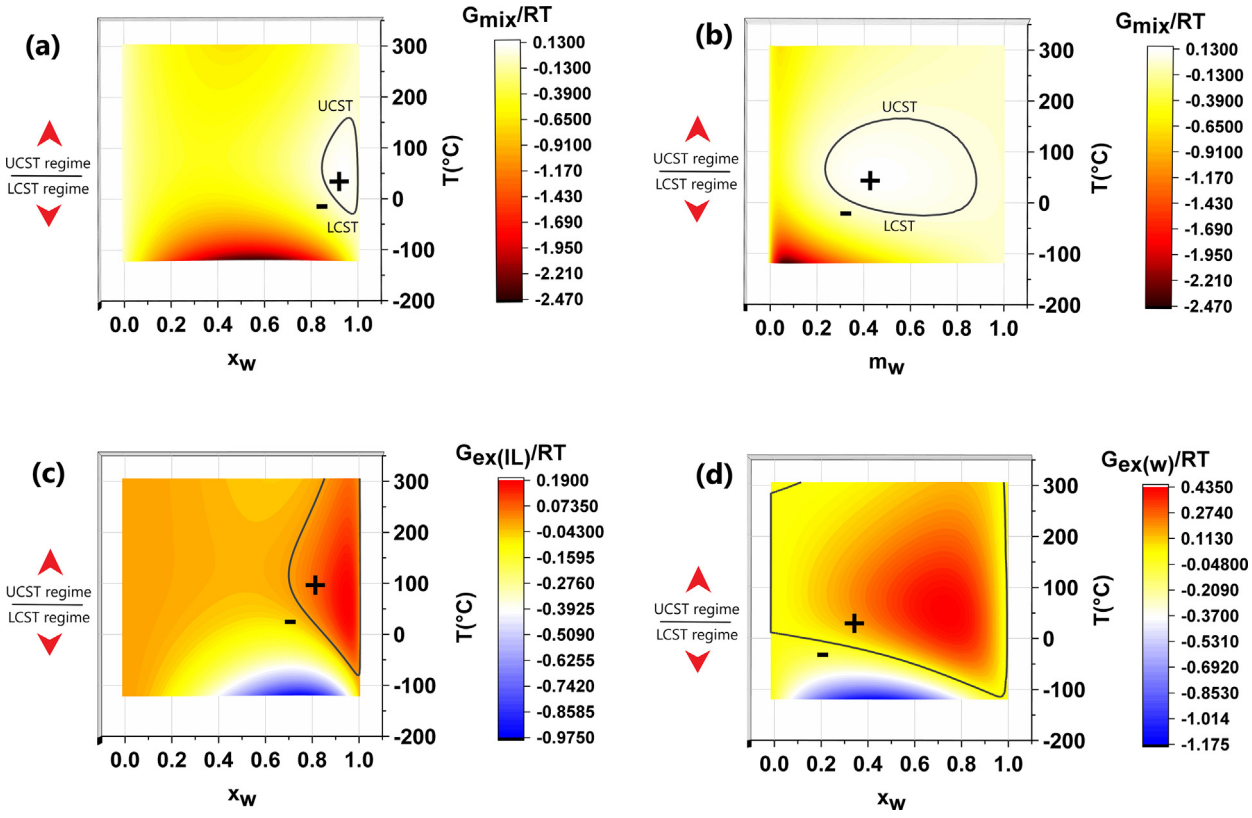

Fig. 3. Phase diagram and Gibbs energy analysis of aqueous $[N_{4444}][SCN]$ solution. Total solution Gibbs energy of mixing plotted with respect to **(a)** water mole fraction and **(b)** water mass fraction. Excess Gibbs free energy of **(c)** $[N_{4444}][SCN]$ ionic liquid and **(d)** water. "**+**" and "**-**" signs delineate regions exhibiting positive and negative excess/mixing Gibbs energy.

ature ≈ 50 °C. Beyond this temperature, as the solution enters UCST regime, the interaction behavior is reversed, and the respective excess contributions begin to decrease with the increase in temperature. As a result, *IL-W* interactions are favored over *IL-IL* and *W-W* interactions, leading to UCST driven phase homogenization. Consequently, overlapping of the respective maxima of the excess Gibbs energies and the associated positive regions results in the overall solution instability ($\boldsymbol{G_{mix}/RT} > 0$), as discussed previously.

Furthermore, it can also be noted that the magnitude of $\boldsymbol{G_{ex}(w)/RT}$ is greater than $\boldsymbol{G_{ex}(IL)/RT}$ in both the regimes. In fact, at their respective peak values (both at ≈ 50 °C) within the unstable region, the magnitude of $\boldsymbol{G_{ex}(w)/RT}$ is more than twice the maximum value of $\boldsymbol{G_{ex}(IL)/RT}$**.** Consequently, the rate of change of $\boldsymbol{G_{ex}(w)/RT}$ with respect to temperature is greater than that of $\boldsymbol{G_{ex}(IL)/RT}$, Therefore, water exhibits greater sensitivity to temperature changes than the IL and plays a pivotal role in governing the thermo-responsiveness of the entire solution.

Finally, it can also be noted that in the LCST regime, water exhibits a positive $\boldsymbol{G_{ex}(w)/RT}$ only in limited (partial) composition range, encompassing the unstable region. This is contrary to the exhibition of a positive $\boldsymbol{G_{ex}(w)/RT}$ across the entire (complete) composition range in the UCST regime. This behavior was found to be consistent across a broad spectrum of ILs that were experimentally verified to exhibit LCST and UCST with water and other solvents such as alcohols (Refer SI pp. 25–83). Thus, the composition range in which positive $\boldsymbol{G_{ex}/RT}$ of the solvent (water/alcohol) is exhibited can also act a predictive and differentiating metric for LCST/UCST behavior. The preceding analysis has been summarized in Table 1. For each phase transition regime and respective excess Gibbs energies, the terms "partial/complete" have been used to delineate type of composition span (range of x_W) over which the positive or negative values are exhibited.

A typical example of water destabilizing the thermodynamic equilibrium of separated phases can be well observed in LCST exhibiting solutions, wherein the positive contribution of $\boldsymbol{G_{ex}(w)/RT}$ decreases as the temperature is lowered. This entails that *W-IL* interactions would take precedence over *W-W* and *IL-IL* interactions, leading to phase homogenization. Kinetically, this can be observed from Fig. 4(b-f) wherein the concentration fluctuations originate in the separated water layer (post LCST) at the top as small-scale perturbations, and continue to grow in amplitude as the solution is cooled, until the fluctuations spread through the entire fluid bulk and mark the onset of cloud phase. Upon further cooling, the cloud phase disappears as phase homogenization concludes.

3. Derivative analysis

The condition for a system of *n*-components to exhibit critical behavior is given by the following Jacobians [18]:

$$J_1 = \frac{\partial(\mu_1, \mu_2 \cdots\cdots \mu_{n-1})}{\partial(x_1, x_2, \cdots\cdots x_{n-1,})} = 0,$$

$$J_2 = \frac{\partial(J_1, \mu_2 \cdots\cdots \mu_{n-1})}{\partial(x_1, x_2, \cdots\cdots x_{n-1,})} = 0$$

For a two component solution, with the substitution of $\mu_i = \frac{\partial G_i}{\partial x_i}|_{T,P,n_{j\neq i}}$, solving the above Jacobians yields the criterion for the existence of a critical point [18]:

$$\frac{\partial^2(G_{mix})}{\partial x_i^2}\Big|_{T,P,n_{j\neq i}} = \frac{\partial^3(G_{mix})}{\partial x_i^3}\Big|_{T,P,n_{j\neq i}} = 0\,,\ \text{which can be restated as}$$

Table 1
Summary of ideal and excess Gibbs energy contributions of water and IL ([N_{4444}][SCN]).

Phase transition regime	$G^{id}_{mix}(IL)/RT$	$G^{id}_{mix}(w)/RT$	$G_{ex}(IL)/RT$	composition range (x_W) in which $G_{ex}(IL)/RT$ is exhibited	$G_{ex}(w)/RT$	composition range (x_W) in which $G_{ex}(w)/RT$ is exhibited
LCST	< 0	< 0	< 0	partial	< 0	partial
			> 0	partial	> 0	partial
UCST	< 0	< 0	< 0	partial	> 0	complete
			> 0	partial		
Effect on the stability of the homogenous solution:	Always increases for all compositions		Decreases in the vicinity of the unstable region for both UCST and LCST regimes		Decreases in the vicinity of the unstable region in the LCST regime Always decreases for all compositions in the UCST regime	

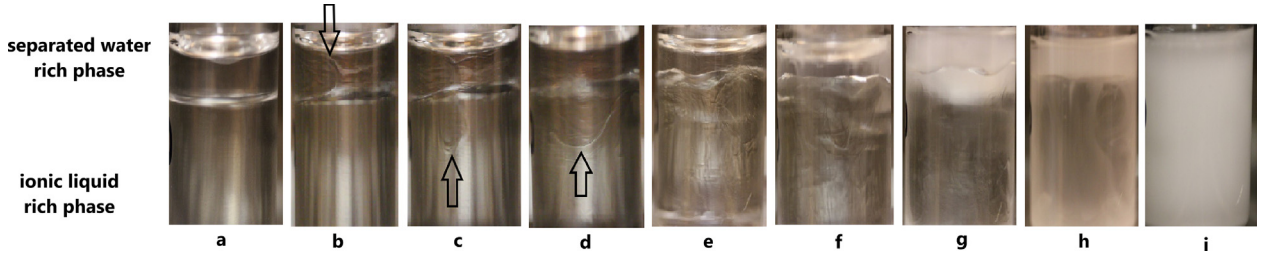

Fig. 4. Concentration fluctuations in phase separated aqueous [P_{4444}][CF_3CO_2] (Tetrabutylphosphonium Trifluoroacetate) as $G_{ex}(w)/RT$ becomes less positive and eventually negative with the decrease in temperature. **(a)** phase separated state **(b)** perturbations originating in water rich phase **(c)** perturbations pass into the ionic liquid rich phase **(d-f)** perturbations grow in amplitude forming concentration fluctuations which spread through the entire fluid bulk **(g-i)** fluctuations subside, marking the onset of cloud phase. Full video clip is available with the SI.

$$\left.\frac{\partial^2(G_{mix}/RT)}{\partial x_i^2}\right|_{T,P,n_{j\neq i}} = \left.\frac{\partial^3(G_{mix}/RT)}{\partial x_i^3}\right|_{T,P,n_{j\neq i}} = 0, \text{ at the critical point} \quad \text{(v)}$$

Furthermore, following conditions must be satisfied for phase separation [18]:

$$\frac{\partial(G_{mix}/RT)}{\partial x_i}\Big|_{T,P,n_{j\neq i}} = 0 \quad \text{(vi)}$$

$$\frac{\partial^2(G_{mix}/RT)}{\partial x_i^2}\Big|_{T,P,n_{j\neq i}} < 0. \quad \text{(vii)}$$

Eqs. (v) - (vii) express the Gibbs energy derivatives with concentration as the only independent variable, keeping other thermodynamic variables constant, and they are valid for both UCST and LCST conditions. However, in order to differentiate between UCST and LCST on the basis of scaled Gibbs energy of mixing, its derivative must include temperature dependence together with the concentration dependence. Notably, T does not appear as an independent variable in Eqs. (v) - (vii). Therefore, scaling Gibbs energy of mixing by the product RT and computing its derivative with respect to x_i does not change the overall derivative behavior. However, to evaluate the temperature dependence of the scaled Gibbs energy derivative, the effect of RT as a scaling factor must be considered. Thus, it warrants scaling the standard correlation: $G_{mix} = H_{mix} - TS_{mix}$ with RT, followed by successive differentiation with respect to x_i and T. Consequently, we obtain the mixed derivative $\frac{\partial^3(G_{mix}/RT)}{\partial T \partial x_i^2}\Big|_{P,n_{j\neq i}}$, which represents the slope/gradient of the second derivative ($\frac{\partial^2(G_{mix}/RT)}{\partial x_i^2}\Big|_{T,P,n_{j\neq i}}$), evaluated along the temperature axis. This derivation and the subsequent analysis results have been provided in the SI (Refer SI pp. 2–9).

For the aqueous [N_{4444}][SCN] solution, the first derivative $\frac{\partial(G_{mix}/RT)}{\partial x_i}\Big|_{T,P,n_{j\neq i}}$ is plotted in Fig. 5(a), depicting the points which satisfy Eq.(vi). Furthermore, Fig. 5(b) represents the second derivative plot delineating the homogenous (“**+**”) and phase separated states (“**-**”) of the solution. A 3D view of the second derivative plot is depicted in Fig. 5(c) which elucidates the slope behavior about the immiscible region. Starting at −120 ℃, the slope magnitude decreases and plateaus as the temperature reaches 20 ℃. This point is also known as the double critical point (DCP) [21], which marks the transition between LCST and UCST regimes. The DCP is obtained as the extremum of the surface enclosed by the closed loop phase diagram and parallel (≈ 0 slope) to the Temperature axis. This temperature is designated as DCPT. More details regarding the DCP and associated critical phenomena can be found in the review article by Narayanan and Kumar [22].

Above 20 ℃, the slope increases as it approaches the UCST. For temperatures above UCST, the slope decreases and asymptotically approaches 0. This behavior, in the immiscible region and its vicinity, is in good agreement with the theoretical analysis findings (Refer SI Tables S1 and S2, pp.8–9) and has been summarized in Eq.(viii) and (ix):

$$\left.\frac{\partial^3(G_{mix}/RT)}{\partial T \partial x_i^2}\right|_{P,n_{j\neq i}} = \begin{cases} < 0 & for\ LCST < T < DCPT \\ 0 & at\ DCPT \\ > 0 & for\ DCPT < T < UCST \end{cases} \quad \text{(viii)}$$

Moreover, behavior of the mixed derivative in homogenous domain, away from the critical points, can be summarized as:

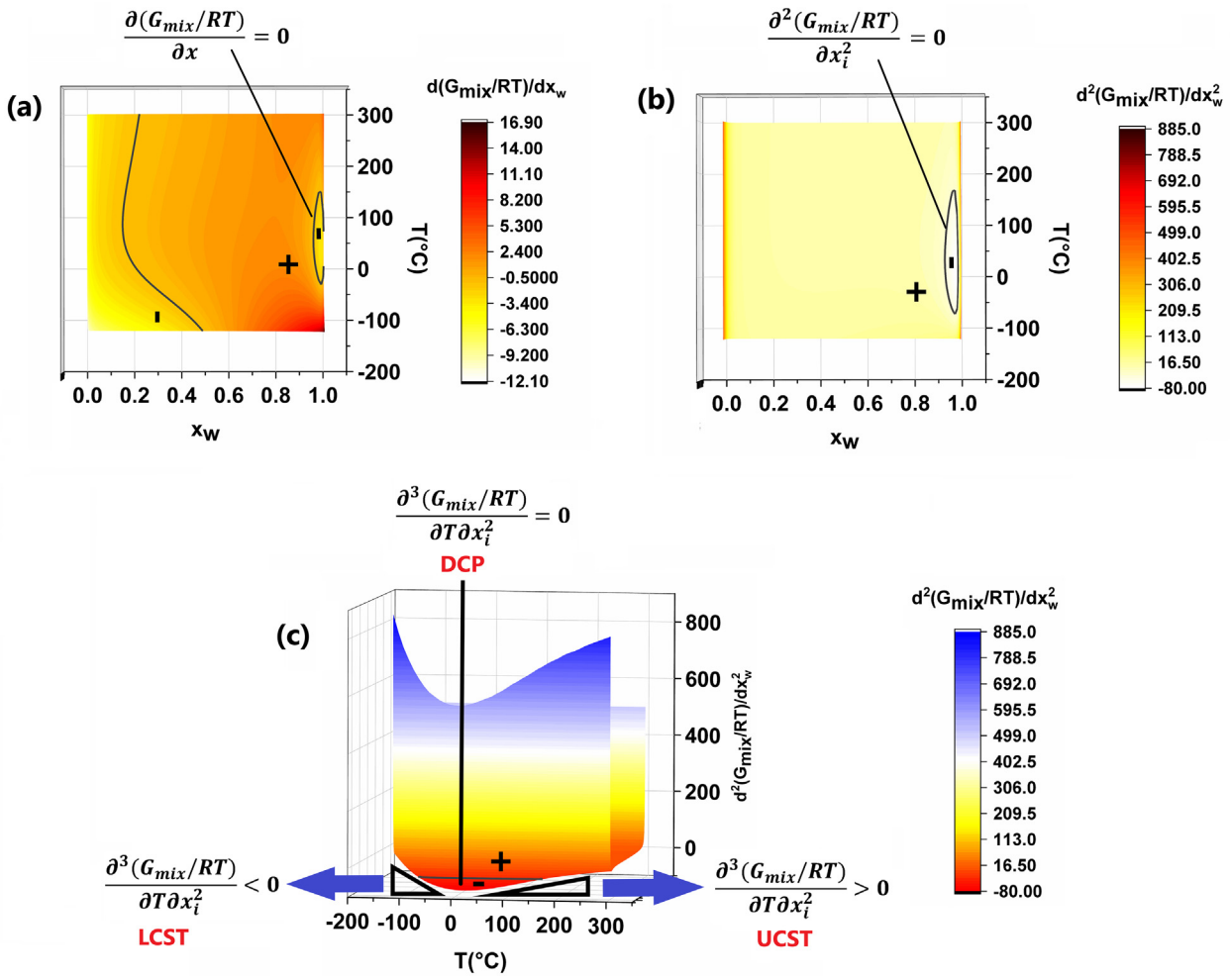

Fig. 5. Gibbs energy of mixing plots for aqueous $[N_{4444}][SCN]$ solution **(a)** variation of 1st derivative of the Gibbs energy, **(b)** and **(c)** variation of 2nd derivative of the Gibbs energy. "**+**" and "**-**" signs delineate regions exhibiting positive and negative values of the 1st and 2nd derivatives.

$$\left.\frac{\partial^3(G_{mix}/RT)}{\partial T \partial x_i^2}\right|_{P,n_{j\neq i}} = \begin{cases} \to -\infty \; for \; T < LCST \\ \to 0 \quad for \; T > UCST \end{cases} \tag{ix}$$

Therefore, LCST can be described as the lowest temperature at the critical concentration for which Eq. (v) is satisfied in the region where the slope, defined by the mixed derivative, is < 0. Similarly, UCST is the highest temperature at the critical concentration for which Eq. (v) is satisfied in the region where the slope is > 0. While the temperature independent conditions for LCST and UCST are mathematically the same, a contrasting behavior is seen in the gradient of the second derivative as the temperature is varied, about the immiscible region.

The third derivative $\left.\frac{\partial^3(G_{mix}/RT)}{\partial x_i^3}\right|_{T,P,n_{j\neq i}}$ plot is represented in in Fig. 6(a), depicting the points which satisfy the condition $\left.\frac{\partial^3(G_{mix}/RT)}{\partial x_i^3}\right|_{T,P,n_{j\neq i}} = 0$. The second derivative plot has been superimposed over the third derivative plot with 50% transparency, as depicted in Fig. 6(b). Due to the highly skewed nature of the phase diagram, both the plots have been plotted in terms of the water mass fraction. This superposition facilitates the visual representation of the condition $\left.\frac{\partial^2(G_{mix}/RT)}{\partial x_i^2}\right|_{T,P,n_{j\neq i}} = \left.\frac{\partial^3(G_{mix}/RT)}{\partial x_i^3}\right|_{T,P,n_{j\neq i}} = 0$, described by Eq. (v) and expedited location of the critical points. In good agreement with the experimental results, UCST of 150°C was located at the critical composition of $m_w \approx 52\%$, whereas LCST could not be precisely located at this composition. The latter result is also consistent with the literature data since it was reported that a unique LCST value could not be determined experimentally [8]. Furthermore, this behavior was attributed to the slow kinetics at very low temperatures (≈ -30 °C), even though LCST type behavior was clearly observed below 20 °C.

4. Reduced activity coefficient

From the excess Gibbs free energy analysis of IL-water systems, the water molecule plays a pivotal role in LCST and UCST driven phase separation by exhibiting a large positive $\boldsymbol{G_{ex}(w)/RT}$ in both cases. Furthermore, there is a characteristic behavior in terms of $\boldsymbol{G_{ex}(w)/RT}$, wherein it is positive in the UCST regime and assumes both positive and negative values in the LCST regime. Since $\boldsymbol{G_{ex}(w)/RT}$ depends upon the water activity coefficient as the sole molecule specific parameter, it is possible to differentiate between LCST and UCST based on the water activity coefficient. Furthermore, Lachwa et al. [23] had asserted that the solvent infinite dilution activity coefficient increased with the increasing temperature for LCST exhibiting solutions. We found that this behavior was emulated in the concentration and temperature dependent solvent activity coefficient too and vice versa for UCST exhibiting solutions. Hence, scaling of the temperature and concentration dependent activity coefficient with respect to the limiting value at infinite

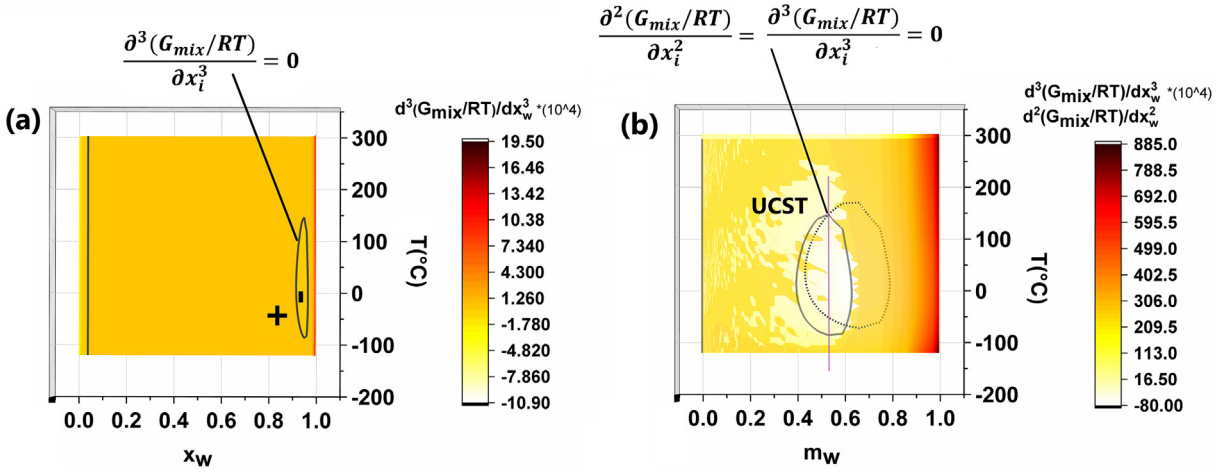

Fig. 6. **(a)** Variation of 3rd derivative of the Gibbs energy of mixing for aqueous $[N_{4444}][SCN]$ solution. "**+**" and "**-**" signs delineate regions exhibiting positive and negative values of the 3rd derivative (**b**) 2nd and 3rd derivatives plotted together (2nd derivative as the top layer with 50% transparency in terms of water mass fraction (m_w).

dilution would result in a generalized metric for predicting LCST/UCST behavior.

Thus, we introduce the dimensionless parameter of Reduced Activity coefficient (Υ_r) defined as:

$$\Upsilon_r = \frac{\Upsilon_i^{\infty}}{\Upsilon_i} \tag{x}$$

$$\Upsilon_r = \begin{cases} < 1 \textit{ in the LCST regime} \\ 1 \qquad \textit{at the DCPT} \\ > 1 \textit{ in the UCST regime} \end{cases} \tag{xi}$$

wherein Υ_i is the solvent activity coefficient at the given T-x in the solution and Υ_i^{∞} is the solvent activity coefficient at infinite dilution at the same temperature. This parameter has been used to delineate the LCST and UCST exhibiting regimes, as depicted in Fig. 7(a) and (b) for aqueous $[N_{4444}][SCN]$ solution. Within computational errors, RAC of ≈ 1.0 is the critical value beyond which this system would not undergo phase separation through LCST. Alternatively, an IL-water binary system would exhibit UCST phase separation at those temperature and concentration coordinates at which $\Upsilon_r > 1$. Another noteworthy point regarding the RAC is that a value of $\Upsilon_r = 1.0$ (at T $\approx$ 20 ^{0}C) coincides with the DCP where $\frac{\partial^3(G_{mix}/RT)}{\partial T \partial x_i^2}|_{P,n_{j\neq i}} = 0$. Therefore, the renormalized activity coefficient value results in a generalized scaling parameter which can be used as a metric for deducing whether an IL-solvent pair would exhibit UCST or LCST presided phase separation.

Conclusion We have demonstrated an approach to probe the phase separation behavior of IL-water/alcohol solutions resulting in a set of metrics for differentiating LCST/UCST behavior. We have delineated the pivotal role of the solvent in initiating phase separation/homogenization. Furthermore, we have formulated an analytical framework which describes the scaled Gibbs energy behavior in the miscible and immiscible solution domains, independently of the COSMO-RS simulation and corroborated the results. Finally, we have proposed a new predictive metric in terms of single molecule specific parameter i.e. the RAC. The findings presented in this study would be indispensable for high throughput solute–solvent screening for processes of scientific and industrial importance.

5. Methods

Ionic liquid synthesis and NMR characterization: Synthesis details of experimentally tested ionic liquids and NMR characterization has been provided in the SI (pp. 84 onwards).

Phase separation experiments: Phase separation experiments were carried out by heating ionic liquid–water solution in glass vials placed in temperature-controlled oven. Temperature was monitored through T-type thermocouples (with a precision of ± 0.5^{0}C) and was increased in steps of 5^{0}C with a holding time

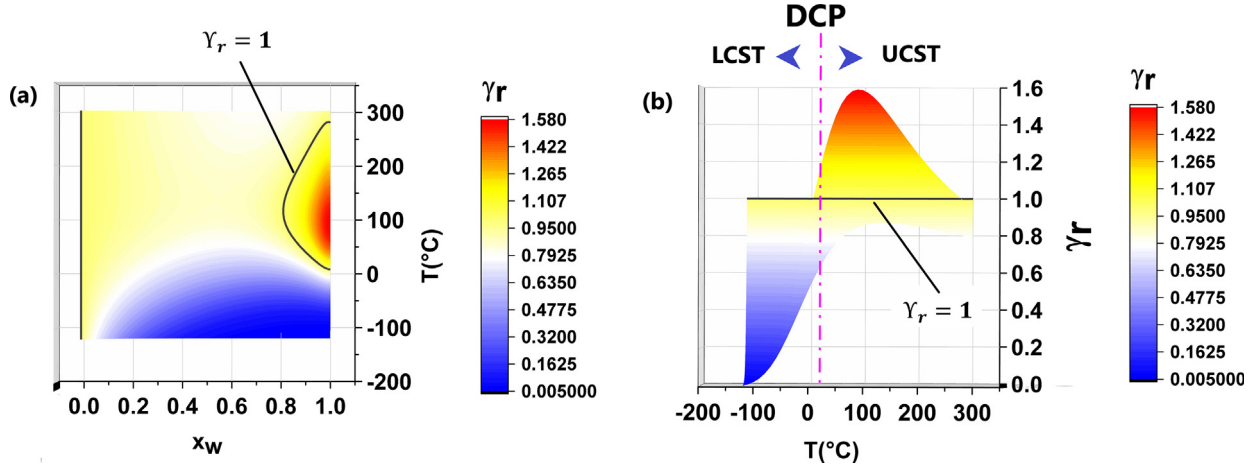

Fig. 7. RAC plotted for aqueous $[N_{4444}][SCN]$ solution **(a)** Top view **(b)** side view.

of 30 min for each temperature step. Phase separation temperature was set as the cloud phase point. Different concentrations of the ionic liquid–water solution were obtained by adding calculated amounts of water depending upon the mass of the ionic liquid to obtain the desired solution concentration.

Molecule construction and equilibrium geometry: Quantum chemical simulations were carried out to optimize the cation–anion pair geometry through Spartan 18 parallel suite. Cation and anion were optimized as a pair of discrete molecules in presence of a solvent with a di-electric constant of 17 (close to that of ionic liquids) using CPCM solvation (Conductor-like polarizable continuum model) model. Density functional method B3LYP with 6–311 + G** basis set was used for molecule geometry optimization. For COSMO-RS activity coefficient computation and sigma profile computation, the molecule geometry optimization was carried out using the GGA: BP86 XC functional, Scalar Relativity with TZP basis set and a small frozen core.

Activity coefficient computation: COSMO-RS (Conductor like screening model for Real solvents) [24] provided by Amsterdam Modelling Suite (AMS 2019.3 COSMO-RS, SCM, Theoretical Chemistry, Vrije Universiteit, Amsterdam, The Netherlands, https://www.scm.com) was used for the estimation of activity coefficients in ionic-liquid water solution at 1.0 ^{o}C temperature intervals with a mole fraction range of 0.0–1.0.

Numerical differentiation: Numerical differentiation was carried out using the following central difference algorithm for discrete data: $f'(x) = \frac{dy}{dx} = 0.5\left(\frac{y_{i+1}-y_i}{x_{i+1}-x_i} + \frac{y_i-y_{i-1}}{x_i-x_{i-1}}\right)$.

Code and 3D plot generation: All graphs have been created using Origin Pro 2018b by OriginLab Corporation.

Data and materials availability: Thermodynamic simulation data with experimental/literature corroboration[25–34], have been provided in the article and the SI. Raw data for the simulation and experiments is also available upon request addressed to the authors.

CRediT authorship contribution statement

Sidharth Sanadhya: Conceptualization, Data curation, Formal analysis, Investigation, Methodology, Project administration, Resources, Software, Validation, Visualization, Writing – original draft, Writing – review & editing. **Zachary D. Tucker:** Conceptualization, Data curation, Formal analysis, Investigation, Methodology, Project administration, Resources, Software, Validation, Visualization, Writing – original draft, Writing – review & editing. **Eva M. Gulotty:** Conceptualization, Data curation, Formal analysis, Investigation, Methodology, Project administration, Resources, Software, Validation, Visualization, Writing – original draft, Writing – review & editing. **William Boggess:** Conceptualization, Data curation, Formal analysis, Investigation, Methodology, Project administration, Resources, Software, Validation, Visualization, Writing – original draft, Writing – review & editing. **Brandon L. Ashfeld:** Conceptualization, Data curation, Formal analysis, Investigation, Methodology, Project administration, Resources, Software, Validation, Visualization, Writing – original draft, Writing – review & editing, Supervision, Funding acquisition. **Saeed Moghaddam:** Conceptualization, Data curation, Formal analysis, Investigation, Methodology, Project administration, Resources, Software, Validation, Visualization, Writing – original draft, Writing – review & editing, Supervision, Funding acquisition.

Declaration of Competing Interest

The authors declare that they have no known competing financial interests or personal relationships that could have appeared to influence the work reported in this paper.

Appendix A. Supplementary material

Supplementary data to this article can be found online at https://doi.org/10.1016/j.molliq.2022.119440.

References

[1] Oak Ridge National Laboratory & BCS Inc., Materials for Separation Technology: Energy and Emission Reduction Oppertunities, *U.S. Department of Energy, Office of Energy Efficiency and Renewable Energy, Industrial Technologies Program,* pp.i-iv,3-5,12-16 (2005). https://www1.eere.energy.gov/manufacturing/industries_technologies/imf/pdfs/separationsreport.pdf.

[2] I.C. Kemp, Fundamentals of Energy Analysis of Dryers, Modern Drying Technology. 4 (2014) 1–45.

[3] D. Chugh, K. Gluesenkamp, O. Abdelaziz, S. Moghaddam, Ionic liquid-based hybrid absorption cycle for water heating, dehumidification, and cooling, Appl. Energy 202 (2017) 746–754.

[4] E. Chiavazzo, M. Morciano, F. Viglino, M. Fasano, P. Asinari, Passive solar high-yield seawater desalination by modular and low-cost distillation, Nat. Sustainability 1 (2018) 763–772.

[5] I. Prigogine, R. Defay, Stability and Critical Phenomena. *Chemical Thermodynamics.* pp. 237-239 (Logmans Green and Co. Ltd., 1954).

[6] A.E. Hill, W.M. Malisoff, The mutual solubility of liquids. III. The mutual solubility of phenol and water. IV. The mutual solubility of normal butyl alcohol and water. *Journal of American Chemical*, Society. 48 (1926) 918–927.

[7] I.C. Sanchez, R.H. Lacombe, Statistical Thermodynamics of Polymer Solutions, Macromolecules 11 (6) (1978) 1145–1156.

[8] H. Glasbrenner, H. Weingärtner, Phase separation and critical point of an aqueous electrolyte solution, J. Phys. Chem. 93 (1989) 3378–3379.

[9] K. Fukumoto, H. Ohno, LCST-type phase changes of a mixture of water and ionic liquids derived from amino acids, Angewandte Chemie. Int. Ed. 46 (2007) 1852–1855.

[10] Y. Kohno, H. Ohno, Ionic liquid/water mixtures: From hostility to conciliation, Chem. Commun. 48 (2012) 7119–7130.

[11] Y. Kohno, H. Arai, S. Saita, H. Ohno, Material design of ionic liquids to show temperature-sensitive lcst-type phase transition after mixing with water, Aust. J. Chem. 64 (2011) 1560–1567.

[12] Y. Fukaya, K. Sekikawa, K. Murata, N. Nakamura, H. Ohno, Miscibility and phase behavior of water-dicarboxylic acid type ionic liquid mixed systems, Chem. Commun. 29 (2007) 3089–3091.

[13] Y. Kohno, H. Ohno, Temperature-responsive ionic liquid/water interfaces: Relation between hydrophilicity of ions and dynamic phase change, PCCP 14 (2012) 5063–5070.

[14] T. Ando, Y. Kohno, N. Nakamura, H. Ohno, Introduction of hydrophilic groups onto the ortho-position of benzoate anions induced phase separation of the corresponding ionic liquids with water, Chem. Commun. 49 (2013) 10248–10250.

[15] Y. Qiao, W. Ma, N. Theyssen, C. Chen, Z. Hou, Temperature-Responsive Ionic Liquids: Fundamental Behaviors and Catalytic Applications, Chem. Rev. 117 (2017) 6881–6928.

[16] Y. Deguchi, N. Nakamura, H. Ohno, Thermoresposnsive ionic liquid/water mixtures for separation and purification technologies, Sep. Purif. Technol. 251 (2020) 117286.

[17] J.W. Gibbs, On the Equilibrium of Heterogenous Substances. *Transactions of the Connecticut Academy, **III**.* pp. 108–248 (1875-1876) and pp. 343–524, (1877-1878).

[18] S.M. Walas, *Phase Equilibria in Chemical Engineering.* Ch.7, pp. 343-390, (Butterworth, 1985).

[19] H. Niedermeyer, J.P. Hallett, I.J. Villar-Garcia, P.A. Hunt, T. Welton, Mixtures of ionic liquids, Chem. Soc. Rev. 41 (2012) 7780–7802.

[20] L.E. Ficke, J.F. Brennecke, Interactions of ionic liquids and water, J. Phys. Chem. B 114 (2010) 10496–10501.

[21] A.I. Fisenko, V.L. Kulinskii, N.P. Malomuzh, Nature of double critical points in binary solutions, Phys. Rev. E 69 (2004) 1–12.

[22] T. Narayanan, A. Kumar, Reentrant phase transitions in multicomponent liquid mixtures, Phys. Rep. 249 (1994) 135–218.

[23] J. Lachwa, J. Szydlowski, V. Najdanovic-Visak, L.P.N. Rebelo, K.R. Seddon, M. Nunes da Ponte, J.M.S.S. Esperança, H.J.R. Guedes, Evidence for lower critical solution behavior in ionic liquid solutions. *Journal of American Chemical*, Society. 127 (18) (2005) 6542–6543.

[24] C.C. Pye, T. Ziegler, E. van Lenthe, J.N. Louwen, An implementation of the conductor-like screening model of solvation within the Amsterdam density functional package. Part II. COSMO for real solvents, Can. J. Chem. 87 (2009) 790.

[25] F.M. Maia, O.K. Rodríguez, E.A. Macedo, LLE for (water+ionic liquid) binary systems using [Cxmim][BF4] (x=6, 8) ionic liquids, Fluid Phase Equilib. 296 (2010) 184–191.

[26] P. Nockemann, B. Thijs, S. Pittois, J. Thoen, C. Glorieux, K.V. Hecke, L.V. Meervelt, B. Kirchner, K. Binnemans, J. Phys. Chem. B 110 (2006) 20978–20992.

[27] S. Saita, Y. Kohno, H. Ohno, Detection of small differences in the hydrophilicity of ions using the lcst-type phase transition of an ionic liquid water mixture, Chem. Commun. 49 (2013) 93–95.

[28] Y. Zhao, L. Tian, Y. Pei, H. Wang, J. Wang, Effect of Anionic Structure on the LCST Phase Behavior of Phosphonium Ionic Liquids in Water, Ind. Eng. Chem. Res. 57 (2018) 12935–12941.
[29] L. Moura, L.C. Brown, M. Blesic, J.D. Holbrey, LCST Phase Behavior and Complexation with Water of an Ionic Liquid Incorporating the 5-Phenyltetrazolate Anion, ChemPhysChem 18 (2017) 3384–3389.
[30] Y. Fukaya, H. Ohno, Hydrophobic and polar ionic liquids, PCCP 15 (2013) 4066–4072.
[31] Y. Kohno, Y. Deguchi, H. Ohno, Ionic liquid-derived charged polymers to show highly thermoresponsive LCST-type transition with water at desired temperatures, Chem. Commun. 48 (2012) 11883–11885.
[32] U. Domańska, A. Marciniak, Solubility of Ionic Liquid [emim][PF6] in Alcohols, J. Phys. Chem. B 108 (7) (2004) 2376–2382.
[33] V. Najdanovic-Visak, J.M.S.S. Esperança, L.P.N. Rebelo, M. Nunes da Ponte, H.J.R. Guedes, K.R. Seddon, H.C. de Sousa, J. Szydlowski, Pressure, Isotope, and Water Co−solvent Effects in Liquid−Liquid Equilibria of (Ionic Liquid + Alcohol) Systems, J. Phys. Chem. B 107 (46) (2003) 12797–12807.
[34] M. Abe, K. Kuroda, D. Sato, H. Kunimura, H. Ohno, Effects of Polarity, Hydrophobicity, and Density of Ionic Liquids on Cellulose Solubility, PCCP 17 (48) (2015) 32276–32282.